

Valorization of industrial wastes for the production of glass ceramics

Anna Kritikaki, Dimitra Zaharaki and Kostas Komnitsas*

School of Mineral Resources Engineering, Technical University Crete, Chania, Crete, 73100, Greece

*Corresponding author: komni@mred.tuc.gr, tel: +30 28210 37686, fax: +30 28210 69554

Abstract

In the present experimental study, CaO-Al₂O₃-SiO₂ glass ceramics were produced by mixing four different binary compositions of industrial wastes, namely fly ash, red mud and metallurgical slag. Molten glass was first produced in alumina crucibles at 1300 and 1500°C and then cast in stainless steel moulds. After cooling, glass was pulverized and used for the production of glass ceramics which were prepared in disks and uniaxially pressed at 60 MPa. The chemical composition of the raw materials as well as the sintering temperature affected microstructure, porosity, compressive strength, Vickers hardness and linear thermal expansion coefficient of the produced glass ceramics. The potential leaching of hazardous elements from glass ceramics was investigated by Toxicity Characteristics Leaching Procedure (TCLP) test, their chemical stability was studied by immersion in distilled water, simulated acid rain solution and seawater for a period up to one month, while their structural integrity was assessed according to ASTM standard C1262-10. The use of analytical techniques, namely X-ray Diffraction (XRD), Scanning Electron Microscopy (SEM), Differential Thermal Analysis (DTA) and Fourier Transform Infrared Spectroscopy (FTIR) provided significant insights on the microstructure of glass ceramics.

Keywords

Glass Ceramics, industrial waste, compressive strength, porosity, microhardness

Introduction

Valorization of industrial wastes and by-products has emerged as an important environmental issue since industrial development generates tonnes of hazardous wastes which have high content of toxic elements, including heavy metals and metalloids. Today, the need for the development of efficient management approaches focusing on reduction of the volume of wastes, immobilization of hazardous elements and energy savings is of high priority. Vitrification, which aims at the conversion of wastes into a stable glassy matrix through thermal treatment, has so far attracted significant attention due to its successful application in a variety of wastes including fly ashes, metallurgical, municipal and even radioactive wastes (Aloisi et al. 2006, Erol et al. 2009). Most of the derived glasses exhibit high chemical inertness (Bin Hussain et al. 2014) and noticeable potential for immobilization of hazardous elements (Leroy et al. 2001).

Another advantage of waste vitrification is the production of glass ceramics from the vitrified materials. Glass ceramics are polycrystalline materials produced by controlled crystallization of a glass matrix and typically consist of a crystalline phase (30-95% w/w) and a residual glassy phase. When adjusting different process parameters such as chemical composition, particle size distribution, treatment time and temperature, tailor made glass ceramics for specific applications can be produced. Based on their favourable properties such as high mechanical strength in elevated temperature, high microhardness, high chemical inertness and low thermal expansion coefficient, glass ceramics can become suitable for a variety of applications including, but not limited to, construction materials, ceramic tiles, catalytic supports, lightweight aggregates and sensors (Zhang et al. 2007, Dong et al. 2009, Tang et al. 2014).

Several studies are available in literature investigating vitrification of different wastes. Blast furnace slag was the first silicate waste used as potential raw material for the synthesis of glass ceramics. The end product, called slag sital, was produced from the vitrification of slag via two-stage heat treatment. The use

of fly ash for the production of ceramics with improved mechanical, chemical and physical properties has been also studied (Rincón et al. 1999, Erol et al. 2008, Wang et al. 2014). The microstructure and properties of glass ceramics were studied by Differential Thermal Analysis (DTA) based on the crystallization behaviour of fly ash (Leroy et al. 2001). CaO-Al₂O₃-SiO₂ (CAS) glass ceramics have been produced from incinerator fly ash through combustion and powder sintering (Cheng & Chen 2003). Both processes resulted in the production of ceramics at 900-950°C with good mechanical and physical properties.

In other studies, different wastes have been investigated in order to produce glass ceramics. The effect of the presence of glass cullet and float dolomite in fly ash powder mixtures was studied by Barbieri et al. (1999) and the presence of alkaline-earth elements was found to improve their mechanical properties. The effect of various additives on the properties of glass ceramics made from several silicate wastes has been also studied (Rozenstaucha et al. 2006). Glass ceramics developed using mixtures of fly ash, peat, clay and waste glass exhibited high relative density (2.4 g/cm³) and mechanical strength (72 MPa).

However, the main drawback of the production of glass ceramics using wastes as raw materials is the high temperature required for glass melting. In order to substantially reduce melting temperature and the associated production cost, several approaches were considered by mixing materials of different compositions. Thus, industrial wastes including slags, red mud, galvanic glass microspheres, acid neutralization salts and medical wastes can be mixed with or without the addition of natural raw materials, e.g. clay, alumina – silicon carbide and silica sand to produce glass ceramics with lower production costs, sufficient physical and mechanical properties (e.g. compressive strength as high as 80 MPa) and low content of hazardous elements (Francis et al. 2013, Mymrin et al. 2014).

In the present study, CaO-Al₂O₃-SiO₂ glass ceramics were produced by mixing high calcium fly ash, red mud and low calcium ferronickel slag. Four different binary compositions were tested and the

effect of mineralogy and temperature on microstructure, porosity and mechanical and physical properties was investigated.

Experimental design

Materials

The raw materials used for the production of glass ceramics were: i) fly ash from the thermal power plant of Ptolemais, NW Greece, ii) red mud from “Aluminum of Greece”, Agios Nikolaos, prefecture of Veotia, Greece and iii) electric arc furnace slag from the “LARCO S.A” ferronickel plant, Larymna, prefecture of Lokris, Greece. Table 1 shows the chemical analysis of the raw materials used in the form of oxides and trace elements, as derived from an X-Ray fluorescence energy dispersive spectrometer (XRF-EDS) Bruker-AXS S2 Range Type. Loss on ignition (LOI) was determined by heating raw materials at 1050 °C for 4h.

X-Ray Diffraction (XRD) analysis of raw materials, as well as of glasses and glass ceramics, was carried out using a Bruker D8 Advance diffractometer with a Cu-K α radiation and a scanning range from 3° to 70° 2 θ , with step 0.03° and 4s/step measuring type. Qualitative analysis was performed using the DIFFRACplus Software (Bruker AXS) and the PDF database.

Fly ash used in the present study is classified as class C ($\text{SiO}_2 + \text{Al}_2\text{O}_3 + \text{Fe}_2\text{O}_3 > 50\%$), while the main crystalline phases detected by XRD are portlandite, anorthite, calcite and quartz. Red mud is a by-product of alumina production by the Bayer process, while its volume and composition may vary widely and depend on the type of bauxite treated. Red mud used consists mainly of iron and aluminum oxides. Ferronickel slag consists of forsterite and fayalite (olivines), quartz, anorthite and cristobalite while its amorphous content exceeds 50%. Commercial silica sand, of 98% purity, obtained from Athens, Greece, was also used in some tests.

Table 1. Chemical analysis (% w/w) of raw materials

| Component | Fly ash | Red mud | Slag |
|-------------------------------------|---------|---------|-------|
| Fe ₂ O _{3(tot)} | 5.6 | 41.65 | 43.83 |
| SiO ₂ | 33.4 | 9.28 | 32.74 |
| Al ₂ O ₃ | 13.1 | 15.83 | 8.32 |
| CaO | 31.85 | 10.53 | 3.73 |
| MgO | 3.67 | 1.13 | 2.76 |
| MnO | 0.18 | - | 0.41 |
| Na ₂ O | 0.46 | 2.26 | - |
| K ₂ O | 0.76 | 0.21 | - |
| P ₂ O ₅ | - | 0.12 | - |
| TiO ₂ | 0.71 | 4.73 | - |
| SO ₃ | 6.58 | 0.3 | 0.45 |
| Cr ₂ O ₃ | 0.06 | 0.09 | 3.07 |
| C | - | - | 0.11 |
| Ni (mg/kg) | 460 | 1055 | 1000 |
| Co (mg/kg) | 68 | - | 200 |
| LOI | 2.7 | 12.77 | - |
| Total | 99.13 | 99 | 95.54 |

All materials were ground prior to use in a FRITSCH pulverizer (Germany) and the average particle size was determined by laser particle analysis using a MASTERSIZER S, Malvern Instrument. The mean particle size of the raw materials used for the production of glasses varied from 30 to 45 μm , while for the production of glass ceramics the mean particle size of glasses varied between 30 and 80 μm .

Glass Synthesis

The binary compositions and the experimental conditions used for the synthesis of glasses are shown in Table 2. The presence of fly ash and silica sand enhances the glass forming ability of the mixture, while the

presence of red mud and slag provide Fe which acts as network modifier for the crystalline structure and facilitates the formation of crystalline phases such as diopside, wollastonite and enstatite (Erol et al. 2009). In order to decrease both the melting temperature of the mixture and the viscosity of molten glass, 10% w/w of borax (Sigma Aldrich, Germany) and 10% w/w of sodium carbonate (Fluka, Germany) were also added in two cases. Glass synthesis was carried out in alumina crucibles after heating the mixture for 2 h at 1300 or 1500 °C. Molten glass was cast in stainless steel moulds.

Table 2. Binary compositions and experimental conditions used for glass synthesis

| Composition | PFA(%) | RM (%) | SK (%) | SS (%) | Borax/Sodium Carbonate(%) | Temperature (°C) |
|-------------|--------|--------|--------|--------|---------------------------|------------------|
| 50P50RM | 50 | 50 | - | - | - | 1500 |
| 90P10RM | 90 | 10 | - | - | - | 1500 |
| 90P10SS | 90 | - | - | 10 | 10/10 | 1500 |
| 90P10SK | 90 | - | 10 | - | 10/10 | 1300 |

PFA: Ptolemais fly ash, RM: red mud, SS: silica sand, SK:slag

Glasses were analysed by Differential Thermal Analysis (DTA) to investigate the crystallization process and determine both glass transition (T_g) and crystallization peak temperature (T_c). DTA analysis was performed using a Perkin Elmer Pyris DTA/TG analyser, while samples were heated from 40 to 1200 °C with a constant rate of 10 °C/min.

Glass ceramics production

The pulverized glasses were used as raw materials for the production of glass ceramics. Four different glass ceramics were prepared in disks and uniaxially pressed at 60 MPa (sample dimensions $\varnothing 30$ mm

diameter, $h \sim 15\text{-}25$ mm). The use of pulverized materials improves processing and the functional characteristics of the final products.

The green samples were dried at 110°C and then sintered for 2h at temperatures varying between 800 and 1000°C , with a heating rate of $3^{\circ}\text{C}/\text{min}$. Open porosity and bulk density of the sintered glass ceramics were measured by mercury porosimetry (Micromeritics Autopore IV 9500); measurements were done in triplicate. The standard deviation in all cases was less than 5%. The compressive strength was determined using an MTS 800 load frame as the average of three measurements. Vickers microhardness measurements were performed by FM-800 Future-Tech microhardness tester. Samples were polished using diamond paste and a load of 500 g was selected. To obtain reproducible results 10 indentations were made on each sample. Dilatometric studies of glass ceramics produced after sintering at 900°C were also performed to determine the coefficient of thermal expansion (CTE) between 40 and 600°C on a Netzsch DIL 402C dilatometer.

The functional groups present in glass ceramics were identified using FTIR analysis on KBr pellets (each sample was mixed with KBr at a ratio 1:100 w/w and pressed to obtain a disc) with a Perkin Elmer Spectrum 1000 spectrometer. The microstructure of the samples was determined by Scanning Electron Microscopy (SEM) using a JEOL 6380LV scanning electron microscope equipped with an EDS INCA microanalysis system.

The toxicity of glass ceramics was investigated by subjecting samples to TCLP (Toxicity Characteristics Leaching Procedure) test (US EPA, 1990). The concentration of Cr, Ni, Zn, Cd, Pb and Cu in the extract was determined using an Agilent Technologies 7500c x inductively coupled plasma mass spectrometry (ICP-MS) analyser (Agilent Technologies, Santa Clara, CA, USA).

The chemical stability of glass ceramics was investigated by immersion of samples in distilled water, simulated acid rain ($\text{H}_2\text{SO}_4\text{:HNO}_3$ 60:40 % w/w, pH 3) and seawater for 1 day, 7 days and 1 month. After immersion for the predetermined period the samples were weighted and the weight loss was calculated.

The structural integrity of the specimens was assessed by employing two 48 h freeze-thaw cycles, with -10°C and 80°C as temperature extremes, according to ASTM standard C1262-10. Weight loss and compressive strength have been also determined after the end of the tests.

Results and Discussion

Mineralogy of glass ceramics

Glasses were initially prepared and chemically characterized as shown in Table 3, in order to optimize the process of glass ceramics production. The XRD patterns of glass and glass ceramics produced after sintering of glass powder at different temperatures are presented in Figures 1-4. The patterns indicate that by increasing sintering temperature from 800 to 1000 °C crystalline phases are developed and the relative intensity of the peaks is also increased, while the amorphous content, indicated by the wide shoulder shown between 17-38°, is reduced in accordance with the chemical composition of the raw materials. Addition of 10% w/w silica sand to fly ash for the synthesis of glass (G-90P10SS) causes the formation of diopside, feldspars, brownmillerite and chromite in the respective glass ceramic (GC-90P10SS). The formation of new phases depends on the sintering temperature. It is shown in Figure 1 that at higher sintering temperature (1000°C) diopside and feldspar peaks become more intense while chromite and brownmillerite are also detected in glass ceramics.

When fly ash and slag (90 and 10% w/w, respectively) are used for the synthesis of glass (G-90P10SK) nepheline, brownmillerite and gehlenite are identified at temperature higher than 900 °C in the respective glass ceramic (GC-90P10SK), due to the presence of Si, Ca and Fe in the raw material (Figure 2). Glasses and the respective glass ceramics produced after sintering at 800 °C show higher amorphicity as indicated by the shoulder shown between 17° and 38° 2θ. As temperature increases the intensity of peaks of enstatite and nepheline also increases.

Table 3.Chemical analysis (%) of glasses

| | G-50P50RM | G-90P10RM | G-90P10SS | G-90P10SK |
|--------------------------------|-----------|-----------|-----------|-----------|
| Na ₂ O | 0.13 | 0.52 | 9.22 | 6.32 |
| MgO | 1.74 | 2.14 | 1.96 | 3.70 |
| Al ₂ O ₃ | 22.81 | 18.93 | 6.16 | 8.27 |
| SiO ₂ | 15.94 | 35.91 | 46.96 | 26.53 |
| P ₂ O ₅ | 0.15 | 0.14 | 0.10 | 0.07 |
| SO ₃ | 0.00 | 0.15 | 0.85 | 0.33 |
| K ₂ O | 0.61 | 1.24 | 0.96 | 0.73 |
| CaO | 22.31 | 19.03 | 15.90 | 15.14 |
| TiO ₂ | 3.16 | 1.53 | 0.42 | 0.71 |
| MnO | 0.05 | 0.03 | 0.01 | 0.15 |
| Fe ₂ O ₃ | 24.18 | 6.81 | 4.13 | 16.15 |
| NiO | 0.05 | 0.02 | 0.01 | 0.04 |
| CuO | - | 0.01 | - | - |
| ZnO | 0.01 | - | - | 0.01 |

According to the XRD patterns of G-50P50RM and G-90P10RM glasses and the respective glass ceramics (GC-50P50RM,GC-90P10RM) (Figures 3 and 4, respectively), similar crystalline phases i.e. gehlenite, enstatite and wollastonite are identified. The phases remained after sintering are gehlenite and hematite. Noother crystalline phases (quartz, anhydrite, gibbsite and lime) were detected due to precipitation and dissolution reactions that tookplace during sintering. The amount of glassy phase was decreased in glass ceramics produced after sinteringat 1000 °C, while the intensity of wollastonite and enstatitepeaks has increased. The presence of Na-Fe crystalline phases in glass ceramics is due to the high Fe content in the starting raw materials and is typical ofglass ceramics derived from CaO-Al₂O₃-SiO₂ (CAS) wastes (Ilic et al. 2003, Xu et al. 2010, He et al. 2013).

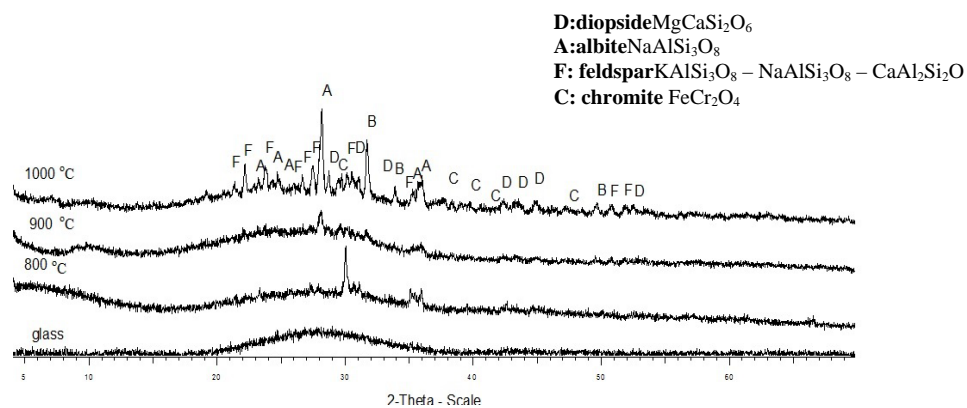


Figure 1. XRD patterns of G-90P10SS glass and the produced glass ceramics (GC-90P10SS) at 800, 900 and 1000°C

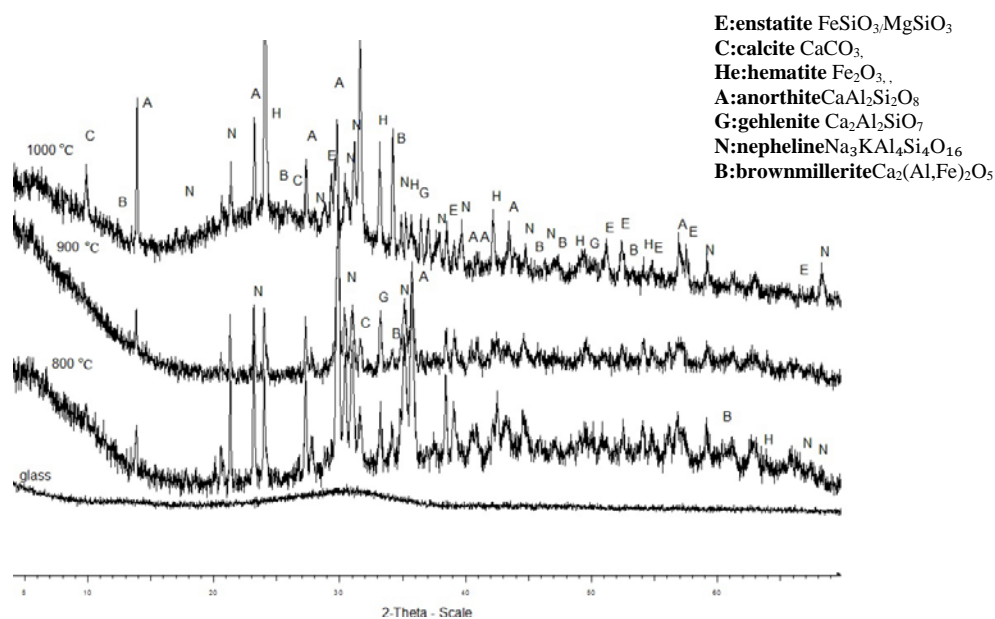


Figure 2. XRD patterns of G-90P10SK glass and the produced glass ceramics (GC-90P10SK) at 800, 900 and 1000°C

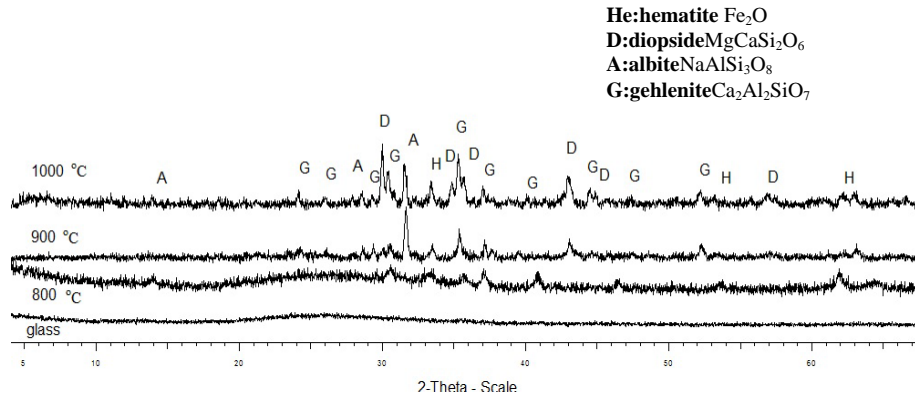


Figure 3. XRD patterns of G-50P50RM glass and the produced glass ceramics (GC-50P50RM) at 800, 900 and 1000°C

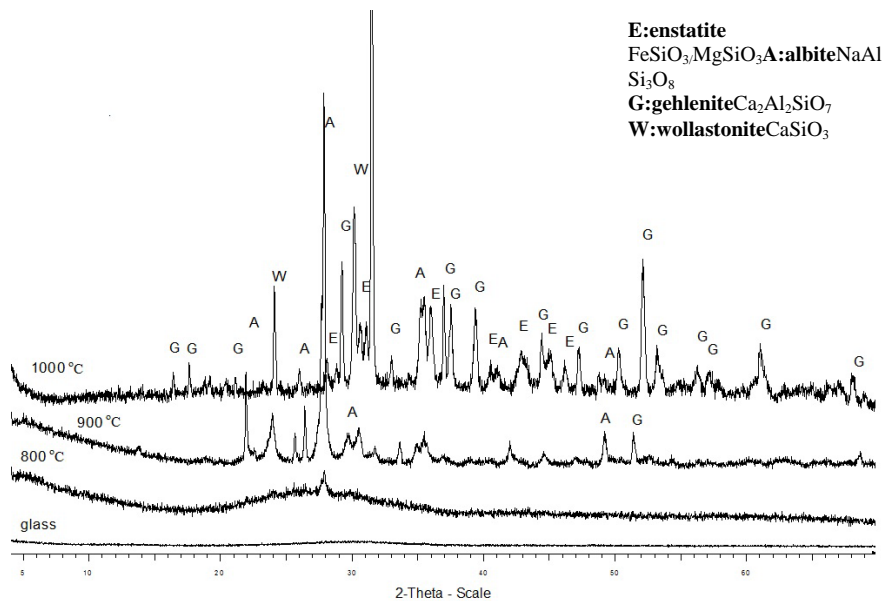


Figure 4. XRD patterns of (G-90P10RM) glass and the produced glass ceramics (GC-90P10RM) at 800, 900 and 1000°C

Microstructure of glass ceramics

Figure 5 presents SEM images and element spectrums (EDS analysis) of glass ceramics produced after sintering at 900 °C of glasses produced from fly ash, red mud and slag. It is shown that in all specimens crystal particles of different size and shape are distributed in a glassy phase. In glass ceramics (GC-90P10SS) produced after sintering of glass produced from fly ash and silica sand, a homogeneous microstructure and a very uniform dispersion of grains into the main glass matrix are shown (Figure 5a). A rigid network of well-connected grains has been developed indicating that this glass exhibits good sinterability. Based on the EDS analysis, shown in Figure 5b, it is deduced that the elongated dark crystals correspond to diopside (D) and the small white grains correspond to chromite (Cr). Figure 5c shows the microstructure of glass ceramics produced after sintering of glass produced from red mud and fly ash (GC-90P10RM), where the amount of glassy phase is uniformly distributed and fills the interparticle voids. Most grains are elongated and the intergrain contact is clearly visible. The needle shaped crystals correspond to wollastonite (W), as also confirmed in Figure 5d. In glass ceramics (GC-90P10SK) produced after sintering of glass produced from fly ash and slag, Figure 5e, it is shown that spherical and laminar shaped grains are uniformly distributed into the glassy phase. Spherical particles varying in size from 2.5 to 5.5 μm correspond to enstatite (E) and laminar particles with a mean particle size of 5 μm to brownmillerite (B), as also deduced from Figure 5f which is similar to Figures 5b and 5d.

The study of the microstructure of glass ceramics produced after sintering of glass at 1000 °C (data not shown) reveals a denser structure where larger particles are embedded into the crystalline matrix. The amount of glassy phase was decreased as sintering temperature increased. In all cases the results are consistent with XRD patterns.

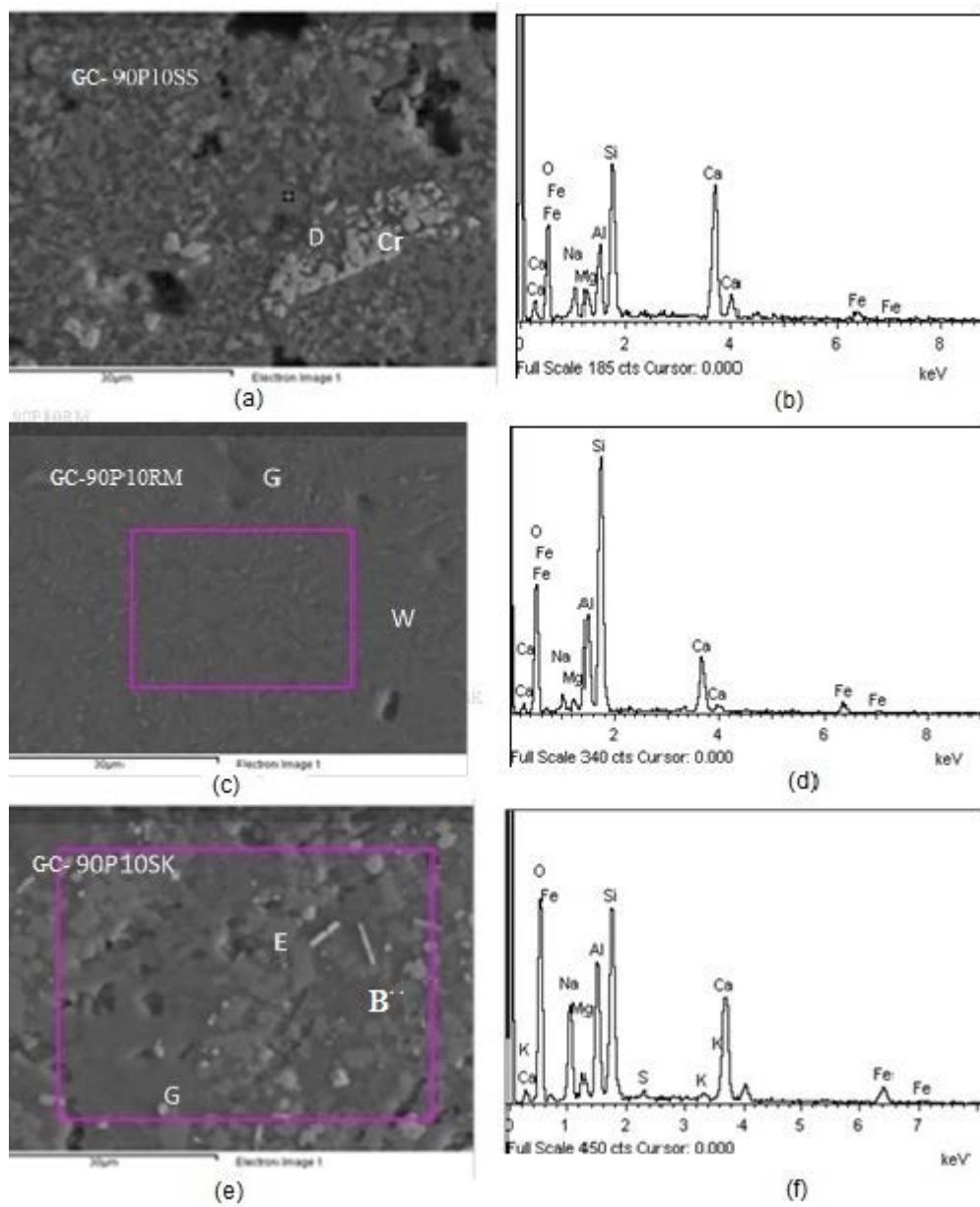


Figure 5. SEM images and elemental spectrums (EDS analysis) of GC-90P10SS (a,b), GC-90P10RM (c,d) and GC-90P10SK (e,f) glass ceramics produced after sintering glass powder at 900 °C

Effect of thermal treatment of glasses

The behaviour of the glass powder during heating was investigated through DTA, where glass transition (T_g) and crystallisation temperatures (T_c) were determined (Figure 6). It is shown that in all samples T_g and T_c strongly depend on composition of raw materials. In glasses with high Fe content (G-50P50RM and G-90P10SK), namely 25% and 15% respectively, the endothermic peaks at 600 and 700 °C indicate the glass transition temperature, while the exothermic peaks at 716 °C for the glass produced from slag and fly ash (G-90P10SK) are probably related to decomposition of calcite. The exothermic peaks around 850 °C, shown in both specimens, are also related to iron content. For the G-90P10RM glass produced from raw materials containing very little red mud a shift of T_c and T_g temperatures to higher values (910 and 820 °C, respectively) is observed.

For the glasses produced from raw materials with higher SiO_2 content (G-90P10SS), T_g is below 600 °C and T_c is at 700 °C. Both temperatures were shifted to lowest values while peaks become more intense when compared to the respective glasses produced from raw materials with high Fe content (G-50P50RM, G-90P10SK). In the latter case T_g is around 700 °C and T_c at 900 °C for G-50P50RM while for the glass G-90P10SK T_g is 630 °C and T_c at 720 °C respectively. The higher temperatures of crystallization and glass transition are evident in G-90P10RM glass where T_g is 850 °C, and crystallization temperature is around 910 °C. This decreasing trend in temperature is also related to the initial particle size of the powdered glass which is around 30 μm for G-90P10SS sample, while for the coarser G-90P10RM sample with a mean particle size of 80 μm , crystallization peak temperature is almost 150 °C higher and reaches 910 °C. Based on the DTA results the selected sintering temperature for all glasses was decided to be 100 °C higher than glass transition temperature to ensure that sinter-crystallization process is completed.

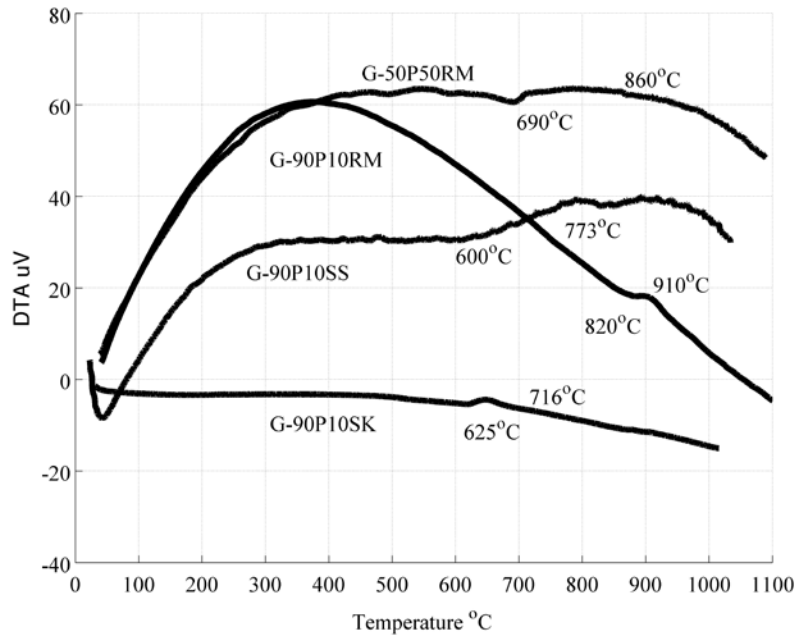


Figure 6.DTA of glasses

FTIR analysis

Figures 7-10 present the FTIR spectra of raw materials, the produced glasses as well as the respective glass ceramics produced at 900°C. The identified FTIR bands are consistent with infrared data of commercial silicate glasses and glass ceramics (Elbatal et al. 2009). The spectra can be divided in three main regions, including high frequency bands between 1000-1100 cm⁻¹, many mid frequency bands between 480 and 700 cm⁻¹, and lower frequency and weaker bands up to 2000 cm⁻¹. The intensity of the peaks of the produced glass ceramics varies depending on the glass composition.

Peaks in glasses containing low SiO₂ and high Al₂O₃ and CaO content as well as in the respective glass ceramics become weaker in high and mid frequency bands, while at low frequency bands show higher intensity (Atalay et al. 2001). The band seen at 480 cm⁻¹ in all glasses can be attributed to the bending motions of the aluminosilicates and the formation of Fe phases. Peak intensity is stronger for glasses with

high Si/Al ratio such as the G-90P10SS. A doublet of peaks between 600 and 800 cm^{-1} is mainly due to Si–O–Si symmetric stretching of bridging oxygen between SiO_4 tetrahedra. The band at around 1000 cm^{-1} is attributed to asymmetric stretching vibrations of the silicate tetrahedral network. The strong band seen at around 1400 cm^{-1} is more dominant for glass ceramics with high Ca content like GC-50P50RM and is due to atmospheric carbonation, asymmetric stretching and out of plane bending modes of CO_3 contained in CaCO_3 (Zaharaki et al. 2010).

Weaker bands shown mostly for glass ceramics at 2400 cm^{-1} are probably due to the presence of Fe phases. Peak intensity gets stronger as Fe content increases, as it is evident for glass ceramics produced after sintering of glasses containing fly ash, red mud and slag (GC-50P50RM, GC-90P10SK). Finally, small bands seen at 3600 cm^{-1} , are associated to stretching vibrations of the –OH bond or to the presence of silanol (SiOH) (Komnitsas et al. 2009). FTIR results of the present study confirm the silicate glass ceramics structure (Liao et al. 2015).

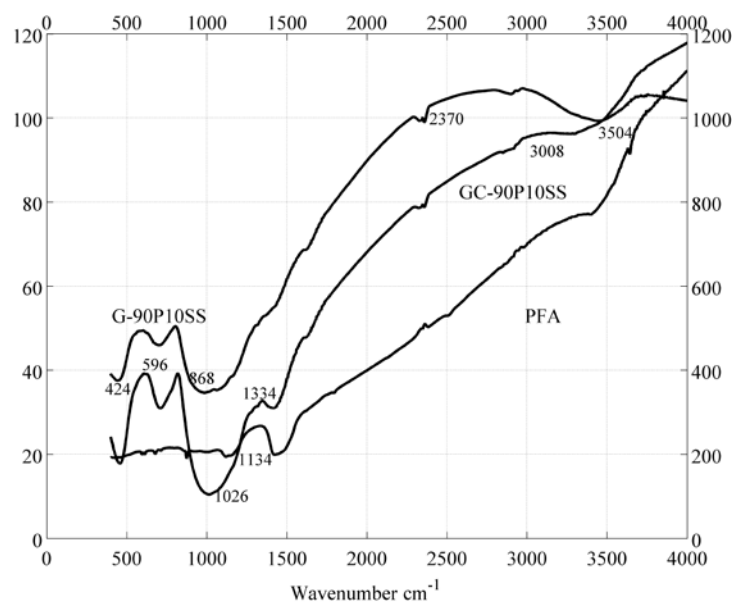


Figure 7. FTIR spectra of Ptolemais fly ash, G-90P10SS glass and GC-90P10SS glass ceramic

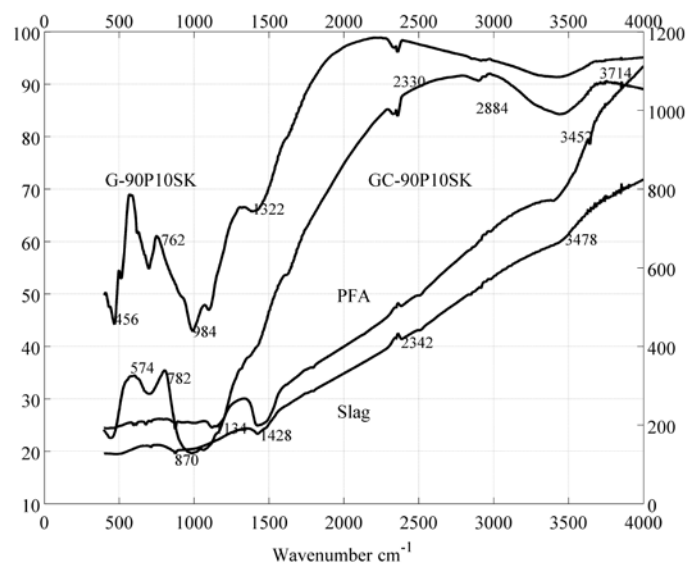


Figure 8. FTIR spectra of Ptolemais fly ash, slag, G-90P10SK glass and GC-90P10SK glass ceramic

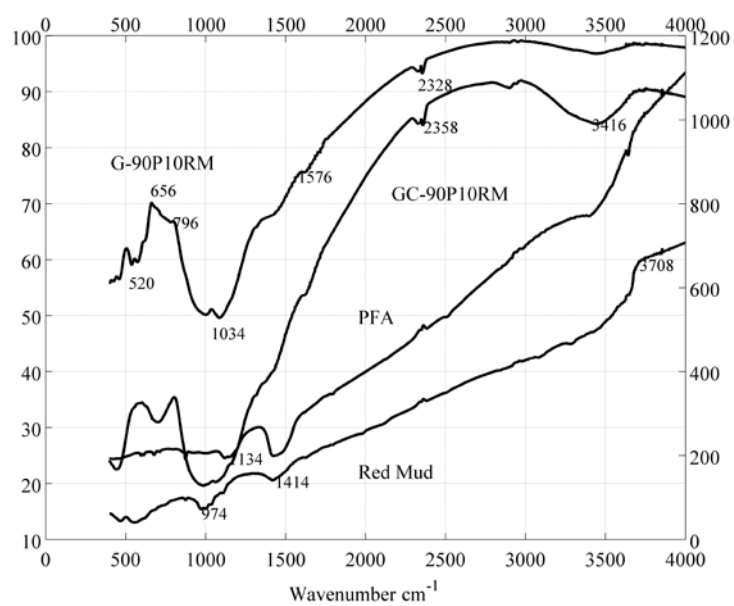


Figure 9. FTIR spectra of Ptolemais fly ash, red mud, G-90P10RM glass and GC-90P10RM glass ceramic

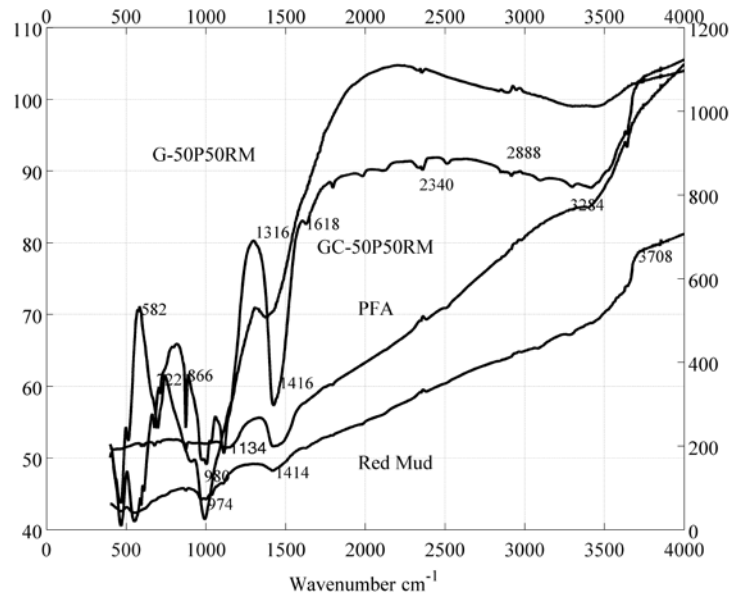


Figure 10. FTIR spectra Ptolemais fly ash, red mud, G-50P50RM glass, and GC-50P50RM glass ceramic

Physical and mechanical properties

The open porosity and bulk density of glass ceramics produced after sintering of glass powder at 800, 900 and 1000 °C, are presented in Table 4. The results indicate that the increase of sintering temperature results in an increase of bulk density and a respective noticeable decrease of porosity for all glass ceramics.

Table 4. Open porosity and bulk density of glass ceramics

| Composition | Open porosity, % | | | Bulk density, g/cm ³ | | |
|-------------|------------------|-------|--------|---------------------------------|-------|--------|
| | 800°C | 900°C | 1000°C | 800°C | 900°C | 1000°C |
| GC-50P50RM | 36.68 | 11.28 | 6.47 | 1.84 | 1.87 | 1.92 |
| GC-90P10RM | 32.29 | 23.03 | 15.66 | 1.84 | 2.02 | 2.13 |
| GC-90P10SS | 31.37 | 2.43 | 2.02 | 1.76 | 2.37 | 2.37 |
| GC-90P10SK | 22.68 | 4.11 | 2.62 | 2.18 | 2.33 | 2.35 |

During sintering of the glass powder, the pores develop intergrain contacts due to diffusion kinetics, thus resulting in densification of the final product and a further decrease of porosity. The better packing of particles, as shown in SEM analysis, results in a more homogeneous structure and in gradual decrease of porosity in the produced glass ceramics. Sintering of powdered glasses, with a mean particle size of 20 μm , also results in better rearrangement of grains, faster diffusion kinetics and early densification. The well-developed crystalline structure of glass ceramics was also observed in XRD patterns. However, glass ceramics produced after sintering of glasses produced from red mud and fly ash, such as GC-90P10RM and GC-50P50RM with high CaO content ($> 20\%$), exhibited higher values of porosity, ranging between 6 and 36%, while the highest value was recorded at the lower sintering temperature. This trend in porosity was also observed in other studies where high residual porosity (30%) was reported in glass ceramics produced from fly ash, silica sand and metallurgical slag (Karamanova et al. 2011, Bin Hussain et al. 2014).

Both open porosity and bulk density of glass ceramics are strongly affected by the chemical composition of the raw materials, their particle size and the degree of crystallization. The low values of porosity, in the range of around 2-4.1 %, were obtained for ceramics, i.e. GC-90P10SS, produced from glasses with high Si/Al ratio (Si/Al: 6.62).

Mechanical properties of glass ceramics, namely compressive strength and Vickers microhardness, were also determined. Compressive strength is affected by the sintering temperature and the particle size of the powdered glass, factors which affect the final microstructure of glass ceramics. As the sintering temperature increases from 800 $^{\circ}\text{C}$ to 1000 $^{\circ}\text{C}$ porosity values decrease and the compressive strength shows a noticeable increase reaching the maximum value of 194 MPa for the glass ceramic produced after sintering of glass produced from fly ash and 10% w/w silica sand (90P10SS) (Table 5).

Table 5. Mechanical properties of glass ceramics

| Composition | Compressive strength (MPa) | | | Vickers microhardness(HV) | | | CTE 20-600°C (10 ⁻⁶ /K) |
|-------------|----------------------------|-------|--------|---------------------------|-------|--------|------------------------------------|
| | 800°C | 900°C | 1000°C | 800°C | 900°C | 1000°C | |
| GC-50P50RM | 21 | 20 | 23 | 257 | 321 | 353 | 2.38 |
| GC-90P10RM | 16 | 49 | 72 | 380 | 447 | 524 | 2.78 |
| GC-90P10SS | 30 | 115 | 194 | 550 | 620 | 732 | 4.91 |
| GC-90P10SK | 10 | 30 | 58 | 584 | 614 | 704 | 1.82 |

Vickers microhardness values are also high for all glass ceramics produced after sintering at 1000 °C. The maximum value, exceeding 730 HV, was obtained for glass ceramic GC-90P10SS indicating that the presence of Si in the raw materials improves substantially both the mechanical and physical properties of the final products. According to He et al. (2013), the increase in the CaO content in glasses results in an increase of both hardness and compressive strength of the produced glass ceramics due to the crystallization of wollastonite which is beneficial for the development of a homogeneous microstructure. This observation is in agreement with the results of the present study where wollastonite is the dominant phase in glass ceramic GC-90P10RM which exhibited high hardness and compressive strength, 524 HV and 72 MPa respectively.

Increase of sintering temperature also resulted in higher values of hardness varying from 257 to 524 HV for specimens produced from raw materials containing red mud (GC-50P50RM, GC-90P10RM), and from 550 HV to 732 HV for glass ceramics produced from raw materials containing slag and silica sand (GC-90P10SS, GC-90P10SK).

Based on the values of porosity (>23%), bulk density (1.84-2.13 gr/cm³) and compressive strength (21-72 MPa) glass ceramics produced from raw materials containing suitable amounts of red mud and fly ash (GC-50P50RM, GC-90P10RM) can be used as filters, catalytic materials and lightweight ceramics. (Shao et al. 2004, Ribeiro & Labrincha 2008, Cetin et al. 2015). According to a previous study (Nanko, 1998) open porosity higher than 30%, high mechanical strength, narrow particle

size distribution and high chemical resistance are required in order to use porous materials as filters and catalysts. On the contrary, glass ceramics produced from silica sand (GC-90P10SS) and slag (GC-90P10SK) exhibiting higher density, lower porosity and high compressive strength may be used as construction materials. Leroy et al. 2001, mentioned that recommended values of density, compressive strength and CTE for commercial bricks are 1.65-2.08 g/cm³, 4.8-27.6 MPa and 4.5-9 10⁻⁶/K respectively, while for building tiles compressive strength should be in the range 26-44 MPa.

Dilatometric studies have been also performed and the coefficient of thermal expansion (CTE) has been determined for the temperature range of 20-600°C. As it is shown in Table 5, CTE values are considered relatively low, while the highest value of 4.91*10⁻⁶/K is obtained for ceramics with the highest alkali content, almost 12 % (GC-90P10SS). These values are consistent with the results obtained by Ribiero et al. (2008), who also observed that the higher CTE are related to the presence of alkalis in the glassy phase.

In Table 6 the main properties of the glass ceramics produced in the present study are compared with the results published in earlier studies indicating the high valorization potential of high calcium fly ash, low calcium ferronickel slag and red mud for the production of glass ceramics with properties suitable for a number of applications.

Potential toxicity of glass ceramics

The TCLP results of the raw materials and the produced glass ceramics, in terms of Cr and Ni which show noticeable leachability in the raw materials, namely fly ash and slag respectively, are presented in Table 7.

Table 6. Comparison of properties of various glass ceramics

| Raw material | Crystallization | Compressive | Density | Porosity | Reference |
|--------------|-----------------|-------------|---------|----------|-----------|
|--------------|-----------------|-------------|---------|----------|-----------|

| | temperature °C | strength MPa | g/cm ³ | % | |
|---|-------------------|-------------------------|-------------------|-------------|------------------------|
| Fly ash | 1150-1200 | | 1.93-3.19 | 0.3-15 | Erol et al. 2008 |
| Fly ash, waste glass | 950-1100 | 26-76 | 1.6-2.2 | | Lu et al. 2014 |
| Fly ash, silica sand | 750-950 | 65-70(bending strength) | 2.9-3 | | Yang et al. 2009 |
| Aluminum waste, waste glass, clay, peat ash | 1080-1180 | 32-42 | 2.5-2.94 | | Lodins et al. 2011 |
| Slag, kaolin, quartz | 1200-1220 | 3-28 | 2.1-2.34 | 39-49 | Karamanova et al. 2011 |
| Fly ash, red mud, silica sand | 910-950 | | 2.8-2.9 | 6-10 | Erol et al. 2000 |
| Fly ash, slag, silica sand, clay | 900-1200 | 20-73 | 1.8-2.68 | 5-35 | Binhussainetal. 2014 |
| <i>Fly ash, red mud, slag, silica sand</i> | <i>800-1100</i> | <i>10-115</i> | <i>1.8-2.35</i> | <i>2-36</i> | <i>Present study</i> |

Table 7.Concentration of heavy metals (mg/L) in the TCLP extract of raw materials and glass ceramics produced after sintering at 900 °C

| Element | GC-50P50RM | GC-90P10RM | GC-90P10SS | GC-90P10SK | Slag | Fly ash | Red mud | US EPA limit |
|---------|------------|------------|------------|------------|-------|---------|---------|--------------|
| Cr | 0.25 | <DL | 0.77 | 2.81 | <DL | 678.9 | <DL | 5 |
| Ni | 0.09 | 0.21 | 0.18 | <DL | 429.5 | <DL | <DL | - |

DL: Detection Limit

It is shown that for both elements their leachability in the produced ceramics is either below detection limit or negligible. The highest concentration, in terms of Cr, is shown for the GC-90P10SK glass ceramic, 2.81 mg/L, which is well below the respective TCLP limit of 5 mg/L. No TCLP limit for Ni is available.

The substantial decrease of leachability of heavy metals in glass ceramics is mainly attributed to the increase in the degree of crystallinity and the entrapment of heavy metal ions in a well-developed crystalline structure (Yang et al. 2009; Vu et al. 2011; Rozenstrauha et al. 2013). The leachability of other

elements such as Cu, Zn, Cd and Pb was not determined since it was below detection limit in the raw materials used.

Structural integrity of glass ceramics

The % weight loss of glass ceramics produced after sintering at 900°C, after immersion in distilled water (pH 6.5), simulated acid rain (pH 3) and seawater (pH 8.2) for 1, 7 and 30 d is shown in Table 8. The results indicate that longer than 7 days immersion period does not result in noticeable increase in weight loss for all specimens and solutions tested. The highest weight loss, as anticipated, was recorded for specimens immersed in simulated acid rain solution, which simulates a highly corrosive environment. The slightly higher weight loss of glass ceramics immersed in sea water, compared to distilled water, is attributed to the effect of chlorine ions present in seawater (Komnitsas et al. 2007).

Table 8. Weight loss (%) of glass ceramics produced after sintering at 900°C

| Specimen | Distilled water | | | Simulated acid rain | | | Seawater | | |
|------------|-----------------|------|------|---------------------|------|------|----------|------|------|
| | 1d | 7d | 30d | 1d | 7d | 30d | 1d | 7d | 30d |
| GC-50P50RM | 1.70 | 1.77 | 2.84 | 4.78 | 5.27 | 6.06 | 3.02 | 4.33 | 5.94 |
| GC-90P10RM | 2.14 | 2.22 | 3.33 | 8.49 | 8.99 | 9.96 | 4.14 | 5.23 | 7.17 |
| GC-90P10SS | 0.88 | 0.92 | 0.98 | 2.78 | 3.39 | 4.16 | 1.27 | 1.44 | 1.56 |
| GC-90P10SK | 0.97 | 1.12 | 2.01 | 3.61 | 4.15 | 5.04 | 1.87 | 2.42 | 2.97 |

Glass ceramics produced from raw materials containing fly ash and red mud (GC-90P10RM, GC-50P50RM and GC-90P10SK), where gehlenite is present in lower or higher percentages, exhibited lower chemical resistance and this is probably due to the gelatinization of gehlenite in acidic solutions (Cheng et al. 2002). The weight loss recorded is mainly attributed to the dissolution of the glassy phase. It

is therefore believed that the chemical stability of the produced glass ceramics depends on the degree of crystallinity and microstructure (Erol et al. 2008, Leroy et al. 2001, Cheng & Chen 2003).

Table 9 shows the compressive strength and the weight loss of glass ceramics subjected to two 48 hours freeze thaw cycles, using -10°C and 80°C as temperature extremes, according to ASTM standard C1262-10.

Table 9. Weight loss and compressive strength of glass ceramics produced after sintering at 900 °C, according to ASTM standard C1262-10

| Specimen | Weight loss, % | Initial Compressive strength, MPa | Final Compressive strength, MPa | Compressive strength loss, % |
|------------|----------------|-----------------------------------|---------------------------------|------------------------------|
| GC-50P50RM | 4.05 | 20 | 15 | 25 |
| GC-90P10RM | 3.11 | 49 | 38 | 22.4 |
| GC-90P10SS | 0.55 | 115 | 106 | 7.8 |
| GC-90P10SK | 2.04 | 30 | 26 | 13.3 |

Measurements show that weight loss is limited for all glass ceramics tested and varies between 0.55 and 4.05%. On the other hand, the loss of compressive strength is rather low for glass ceramics produced after sintering of glass produced from raw materials containing fly ash and either silica sand or slag (GC-90P10SS and GC-90P10SK). The first specimen maintained its compressive strength in remarkable levels (106 MPa). Finally, glass ceramics produced from raw materials containing red mud (GC-50P50RM, GC-90P10RM), although they exhibited low weight loss, exhibited higher loss of compressive strength which varied between 22 and 25%.

Conclusions

Glass ceramics with beneficial properties can be successfully produced through sintering of glasses derived from industrial wastes such as high calcium fly ash, low calcium ferronickel slag and red mud. In the present study, these three wastes were used for the production of glasses at 1300 and 1500 °C which were then pulverized and sintered between 800 and 1000 °C for the production of glass ceramics. The main crystalline phases detected in glass ceramics were wollastonite, enstatite and diopside belonging to CaO-Al₂O₃-SiO₂ (CAS) system. A small amount of glassy phase remained in the matrix at 900 °C, while sintering at 1000 °C results in an increase of crystallinity and intensity of peaks associated mainly with Ca and Fe phases. Crystal particles of 2-5.5 µm were uniformly dispersed into the glassy matrix in all glass ceramics as indicated by the use of analytical techniques.

Sintering temperature affects porosity, microhardness, compressive strength and linear thermal expansion coefficient of the produced ceramics. Also, the increase of sintering temperature results in increase of density, for which the maximum values (~2.35 g/cm³) were acquired for glass ceramics produced from fly ash and silica sand or slag. Glass ceramics prepared from red mud and fly ash, with CaO content higher than 20%, show higher porosity which reaches 36.7%. Despite the increase of porosity, the compressive strength and the Vickers microhardness of all glass ceramics are high reaching 194 MPa and 732 HV respectively for specimen GC-90P10SS, which produced after sintering at 1000 °C. Low thermal expansion coefficient values, in the range of 1.8-4.9*10⁻⁶/K, have been also measured. The concentration of heavy metals in the TCLP extracts of all glass ceramics is either negligible or well below the respective US EPA limits due to the increase of the degree of crystallinity in the final products and the entrapment of heavy metal ions in the crystalline structure. In addition, limited weight loss was recorded for glass ceramics immersed in distilled and seawater, which increased considerably but did not exceed 10% when specimens immersed in simulated acid rain solution. Finally, the loss of compressive strength of glass ceramics subjected to freeze-thaw cycles, according to ASTM standard C1262-10, varied

between 7.8 and 25%. It has to be underlined though that the lower value of compressive strength was 15 MPa (GC-50P50RM), while the higher, although reduced, reached 106 MPa (GC-90P10SS).

Acknowledgements

This research has been co-funded by the European Union (European Social Fund) and Greek National Resources through the Operational Program "Education and Lifelong Learning" of the National Strategic Reference Framework (NSRF) – Research Funding Program: THALES, Sub-project "Development of an integrated methodology for the management, treatment and valorisation of hazardous waste (WasteVal)" (code MIS 380038). Investing in knowledge society through the European Social Fund.

References

- Aloisi, M., Karamanov, A., Taglieri, G., Ferrante, F., & Pelino, M. (2006) Sintered glass ceramic composites from vitrified municipal solid waste bottom ashes. *Journal of Hazardous Materials B*, 137, 138-143
- ASTM C1262-10 (2010) Standard Test Method for Evaluating the Freeze-Thaw Durability of Dry-Cast Segmental Retaining Wall Units and Related Concrete Units. ASTM International, West Conshohocken, PA, www.astm.org.
- Atalay, S., Adiguzel, H.I., & Atalay, F. (2001) Infrared absorption study of Fe₂O₃-CaO-SiO₂ glass ceramics. *Materials Science and Engineering A*, 304-306, 796-799
- Barbieri, L., Lancellotti, I., Manfredini, T., Queralt, I., Rincon, J.M., & Romero, M. (1999) Design, obtainment and properties of glasses and glass-ceramics from coal fly ash. *Fuel*, 78, 271-276
- Binhussain, M.A., Marangoni, M., Bernardo, E., & Colombo, P. (2014) Sintered and glazed glass-ceramics from natural and waste raw materials. *Ceramics International*, 40, 3543-3551
- Cetin, S., Marangoni, M., & Bernardo, E. (2015) Lightweight glass-ceramic tiles from the sintering of mining tailings. *Ceramics International*, 41, 5294-5300

- Cheng T.W., Ueng T.H., Chen Y.S., Chiu J.P. (2002) Production of glass-ceramic from incinerator fly ash. *Ceramics International*, 28, 779-783
- Cheng W., & Chen, Y.S. (2003) On formation of $\text{CaO-Al}_2\text{O}_3\text{-SiO}_2$ glass-ceramics by vitrification of incinerator fly ash. *Chemosphere*, 51, 817-824
- Dong, Y., Zhou, J.E., Lin, B., Wang, Y., Wang, S., Miao, L., Lang, Y., Liu, X., & Meng, G. (2009) Reaction-sintered porous mineral based mullite ceramic membrane supports made from recycled materials. *Journal of Hazardous Materials*, 172, 180-186
- Elbatal, H.A., Ghoneim, A., & Ouis, M.A. (2009) Preparation of glass and glass ceramics from industrial waste materials including slag and cement dust. *Proceedings of the International Conference on Composite Materials ICCM17*, Edinburgh, 27-31 July, pp.1-8
- Erol, J.M., Kucukbayrak, S., & Ersoy-Mericboyu, A. (2008) Comparison of the properties of glass, glass-ceramic and ceramic materials produced from coal fly ash. *Journal of Hazardous Materials*, 153, 418-425
- Erol, J.M., Genc, A., Ovecoglu, M.L., Yucelen, E., Kucukbayrak, S., & Taptik, Y. (2000) Characterization of a glass-ceramic produced from thermal powerplant. *Journal of the European Ceramic Society*, 20, 2209-2214
- Erol, J.M., Kucukbayrak, S., & Ersoy-Mericboyu, A. (2009) The influence of the binder on the properties of sintered glass-ceramics produced from industrial wastes. *Ceramics International*, 35, 2609-2617
- Francis, A.A., AbdelRahman M.K., & Daoud, A. (2013) Processing, structures and compressive properties of porous glass-ceramic composites prepared from secondary by-product materials. *Ceramics International*, 39, 7089-709
- He, F., Tian, S., Xie, J., Liu, X., & Zhang, W. (2013) Research on Microstructure and Properties of Yellow phosphorous Slag Glass ceramics. *Journal of Materials and Chemical Engineering*, 1, 27-31.

- Ilic, M., Cheeseman, C., Sollars, C., & Knight, J. (2003) Minerology and microstructure of sintered lignite coal fly ash. *Fuel*, 82(30), 331-336
- Karamanova, E., Avdeev, G., & Karamanov, A. (2011) Ceramics from blast furnace slag, kaolin and quartz, *Journal of the European Ceramic Society*, 31, 989-998
- Komnitsas, K., Zaharaki, D., Perdikatsis, V. (2007) Geopolymerisation of low calcium ferronickel slags, *Journal of Materials Science*, 42(9), 3073-3082
- Komnitsas, K., Zaharaki, D., & Perdikatsis, V. (2009) Effect of synthesis parameters on the compressive strength of low-calcium ferronickel slag inorganic polymers. *Journal of Hazardous Materials*, 16, 760-768
- Leroy, C., Ferro, M.C., Monteiro, R.C.C., & Fernandes, M.H.V. (2001) Production of glass-ceramics from coal ashes. *Journal of the European Ceramic Society*, 21, 195-202
- Liao Q., Wang F., Kuiru C., Sheqi P., Hanzhen Z., Mingwei L., Jianfa Q. (2015) FTIR spectra and properties of iron borophosphate glasses containing simulated nuclear wastes, 1092, 187-191
- Lodins, E., Rozenstrauha, I., Krage, L., Lindina, L., Drille, M., Filipenkov, V., & Chatzitheodoridis, E. (2011) Characterization of glass-ceramics microstructure, chemical composition and mechanical properties. *Materials Science and Engineering*, 25, 1-10
- Lu, J., Lu, Z., Peng, C., Li, X., & Jiang, H. (2014) Influence of particle size on sinterability, crystallization kinetics and flexural strength of wollastonite glass-ceramics from waste glass and fly ash. *Materials Chemistry and Physics*, 148, 449-456
- Mymrin, V., Ribeiro, R.A.C., Alekseev, K., Zelinskaya, E., Tolmacheva, N., & Catai, R., (2014) Environment friendly ceramics from hazardous industrial wastes. *Ceramics International*, 40(7), Part A, 9427-9437
- Nanko M., Komarneni S., Ishizaki K., (1998) Porous materials, Process technology and applications, pp.3-5, Kluwer Academic Publishers, London

- Ribeiro, M.J., & Labrincha, J.A. (2008) Properties of sintered mullite and cordierite pressed bodies manufactured using Al-rich anodising sludge. *Ceramics International*, 34, 593-597
- Rincón, J.Ma., Romero, M., & Boccaccini, A.R. (1999) Microstructural characterization of a glass and a glass-ceramic obtained from municipal incinerator fly ash. *Journal of Materials Science*, 34, 4413-4423
- Rozenstrauha, I., Lodins, E., Krage, L., Drille, M., Balode, M., Putna, I., Filipenkov, V., Chinnam, R.K., Boccaccini, A.R. 2013 Functional properties of glass-ceramic composites containing industrial inorganic waste and evaluation of their biological compatibility, *Ceramics International*, 39(7), 8007-8014
- Shao, H., Liang, K., Zhou, F., Wang, G., & Peng, F. (2004) Characterization of cordierite-based glass-ceramics produced from fly ash. *Journal of Non-Crystalline Solids*, 337, 157-160
- Tang, B., Lin, J., Qian, S., Wang, J., & Zhang, S. (2014) Preparation of glass ceramic foams from the municipal solid wasteslag produced by plasma gasification process. *Materials Letters*, 128, 68-70
- USEPA (US Environmental Protection Agency), November 1990, Toxicity Characteristics Leaching Procedure (TCLP). Method 1311, Revision 0
- Vu, D.-H., Wang, K.-S., Nam, B.X., Bac, B.-H., Tien-Chun Chu, T.-C. (2011) Preparation of humidity-controlling porous ceramics from volcanic ash and waste glass. *Ceramics International*, 37(7), 2845-2853
- Wang, S., Zhang, C., & Chen, J. (2014) Utilization of coal fly ash for the production of glass-ceramics with unique performances: a brief review. *Journal of Materials Science and Technology*, 30(12), 1208-1212
- Xu, G.R., Zou, J.L., & Li, G.B. (2010) Stabilization of heavy metals in sludge ceramsite. *Water Research*, 44, 2930-2938
- Yang, J., Xiao, B., & Boccaccini, A.R. (2009) Preparation of low melting temperature glass-ceramics from municipal waste incineration fly ash. *Fuel*, 88, 1275-1280

- Zaharaki, D., Komnitsas, K., &Perdikatsis, V. (2010) Use of analytical techniques for identification of inorganic polymer gel composition. *Journal of Material Science*, 45, 2715-2724
- Zhang,J., Dong,W., Li,J., Qiao,L., Zheng,J., &Sheng,J.(2007) Utilization of coal fly ash in the glass–ceramic production. *Journal of Hazardous Materials*, 149, 523-526